Modern Physics Letters B, Vol. 21, No. 28 (2007) 1895–1913

ELASTICITY AND STABILITY OF A HELICAL FILAMENT WITH SPONTANEOUS CURVATURES AND ISOTROPIC BENDING RIGIDITY

ZICONG ZHOU

Department of Physics and Graduate Institute of Life Sciences, Tamkang University, 151 Ying-chuan, Tamsui 25137, Taiwan, R.O.C
Physics Division, National Center for Theoretical Sciences at Taipei, National Taiwan University, Taipei 10617, Taiwan, R.O.C
zzhou@mail.tku.edu.tw

BÉLA JOÓS

Ottawa Carleton Institute for Physics, University of Ottawa Campus, Ottawa, Ontario, Canada, K1N-6N5
http://www.science.uottawa.ca/~ bjoos/
bjoos@uottawa.ca

PIK-YIN LAI

Department of Physics and Center for Complex Systems, National Central University, Chung-li, Taiwan 320, R.O.C
Physics Division, National Center for Theoretical Sciences, 101 Sec. 2 Kuang Fu Road, Hsinchu, Taiwan 300, R.O.C
pylai@phy.ncu.edu.tw

YUAN-SHIN YOUNG and JENG-HUEI JAN

Department of Physics, Tamkang University, 151 Ying-chuan, Tamsui 25137, Taiwan, R.O.C

Received 14 July 2007
Revised 24 July 2007

We derive the shape equations in terms of Euler angles for a uniform elastic rod with isotropic bending rigidity and spontaneous curvature, and study within this model the elasticity and stability of a helical filament under uniaxial force and torque. We find that due to the special requirements on the boundary conditions, a static slightly distorted helix cannot exist in this system except in some special cases. We show analytically that the extension of a helix may undergo a one-step sharp transition. This agrees quantitatively with experimental observations for a stretched helix in a chemically-defined lipid concentrate (CDLC). We predict further that under twisting, the extension of a helix in CDLC may also exhibit similar behavior. We find that a negative twist tends to destabilize a helix.

Keywords: Elasticity; biopolymer; helix; filament.

PACS Number(s): 46.32.+x, 46.25.Cc, 62.20.Fe, 87.15.Ya, 05.40.-a

1. Introduction

The study of a long thin rod (i.e., a filament) has a long history in mechanics and engineering dating back to Euler and Lagrange.[1,2] It has an increasing importance due to recent experiments and theories which revealed its relevance to microscopic objects such as carbon nanotubes[3–8] and biomaterials.[9–42] In a first approximation, a rod can be viewed as an inextensible chain with a certain bending rigidity but with negligible cross-section. This is called the worm-like chain (WLC) model.[24–27] The WLC model has been used to predict a biopolymer's elastic response successfully in the low force regime. But the WLC model cannot account for the behavior of a rod under twisting. The next approximation is to regard the rod as a chain with a spontaneous twist and a circular cross-section which ensures an isotropic bending rigidity. The corresponding model is often referred to as the worm-like rod chain (WLRC) model.[23–31] The WLRC model has been applied successfully to explain the supercoiling properties of double stranded DNA (dsDNA). But the WLRC model cannot yield a free standing helix, that is a helix free of force and torque. To describe a rod which can form a free standing helix, it is necessary to consider a model with spontaneous curvatures,[1,43,44] and this is the model we will investigate in this work.

Of all the possible conformations of a rod, the helix is in general the first one to be studied due to its simplicity and it is one of the most common filamentary structures found in nature. In this paper, we attempt to provide a full picture of the elasticity of a helical rod within a model with spontaneous curvatures and twist. We have presented a brief report on the elasticity of a helical rod under fixed torque in a more general model, i.e. a rod with spontaneous curvatures, torsion and non-circular cross-section.[45] In Ref. 45, we find that a helical filament may undergo a one-step shape transition in extension under-stretching force, and the corresponding energy-force curve is self-crossed, indicating a metastable regime. In this paper, we present a detailed study on a slightly simplified model, i.e. a filament with a circular cross section. The appeal of the present model is that all variables can be separated completely so the expressions can be simplified greatly, and consequently, it is easy to get a full picture of the physical properties of the filament. Our results agree well with a recent experiment for a helix in a chemically-defined lipid concentrate (CDLC).[39] This experiment observed a one-step reversible sharp transition of extension from an almost perfect helix, to an almost straight line, and there is a metastable regime, in which upon nucleation, the helix separates into two domains, one straight and the other helical.[39] Moreover, the elasticity and stability of a twisted helical filament with fixed force does not seem to be available and so we present a detailed discussion of this important issue in this work.

There are in general two ways to study the behavior of a filament. The statistical mechanical treatment is used to find many useful quantities such as the mean chain extension and correlation functions. However, such an approach provides only averaged quantities and some important information such as the shape of the filament is not available. On the other hand, the classical mechanical method[18,20,21,23] can provide some additional insights, and such a treatment is reasonable if thermal fluctuations are negligible, such as when the persistence length of the helix is comparable to the length of the filament, which is the case for the experiments we will discuss.[39]

In this paper, we derive the shape equations for a uniform rod with a circular cross-section in terms of Euler angles θ, ϕ and ψ. We find that to form a helix, the Euler angle ψ must be a constant determined by the spontaneous curvatures. From the boundary conditions, we find that in general, a static, slightly distorted helix cannot exist in this model, though dynamically it is still possible. The elastic response and stability of a helix under different constraints are also studied. We find that negative twisting (unwinding) tends to destabilize a helix. We find that the extension of a helix may be subject to a one-step sharp transition. Especially, we predict that under twisting, the extension of the helix in CDLC can undergo a sharp transition.

This paper is organized as follows. The following section introduces the model and derives the shape equations of the helical filament. Section 3 presents our results under external force and torque. A summary concludes the paper.

2. Shape Equations of the Model

Using arclength s as the variable, the configuration of a uniform rod can be described by a triad of unit vectors $\{\mathbf{t}_i(s)\}_{i=1,2,3}$, where $\mathbf{t}_3 \equiv d\mathbf{r}/ds$ is the tangent to the center line $\mathbf{r}$ of the rod, and $\mathbf{t}_1$ and $\mathbf{t}_2$ are oriented along the principal axes of the cross-section. The orientation of the triad as one moves along the filament is given by the solution of the generalized Frenet equations that describe the rotation of the triad vectors, $d\mathbf{t}_i(s)/ds = -\Sigma_{j,k}\epsilon_{ijk}\omega_j(s)\mathbf{t}_k(s)$, where ϵ_{ijk} is the anti-symmetric tensor, and $\{\omega_j(s)\}$ are the curvature and torsion parameters. Using Euler angles $\theta(s)$, $\phi(s)$ and $\psi(s)$[46] to relate the fixed coordinate system to the frame rigidly embedded in the rod in its relaxed configuration,[19–21,23,34] we can write $\mathbf{t}_3 = \{\sin\phi\sin\theta, -\cos\phi\sin\theta, \cos\theta\}$, and the normal $\mathbf{n} = \{\cos\phi\cos\psi - \cos\theta\sin\phi\sin\psi, \sin\phi\cos\psi + \cos\theta\cos\phi\sin\psi, \sin\theta\sin\psi\}$. It follows that

$$\omega_1 = \sin\theta\sin\psi\dot{\phi} + \cos\psi\dot{\theta}\,, \tag{1}$$

$$\omega_2 = \sin\theta\cos\psi\dot{\phi} - \sin\psi\dot{\theta}\,, \tag{2}$$

$$\omega_3 = \cos\theta\dot{\phi} + \dot{\psi}\,, \tag{3}$$

where the symbol "$\dot{}$" represents the derivative with respect to s.

The energy of a uniform rod with spontaneous curvatures ω_{10}, ω_{20} and spontaneous twist rate ω_0, as well as the symmetric bending rigidities can be written as

$$E = \int_0^L \mathcal{E} ds\,,$$

$$\mathcal{E} = \frac{a_1}{2}\left[(\omega_1 - \omega_{10})^2 + (\omega_2 - \omega_{20})^2\right] + \frac{a_3}{2}(\omega_3 - \omega_0)^2 - f\cos\theta - \Gamma\dot{\phi} - \Gamma_\psi\dot{\psi}\,, \quad (4)$$

where a_1 is the bending rigidity and a_3 is the twisting rigidity, f is a uniaxial force and is along the z-axis ($f < 0$ for compression), and Γ is the torque which produces the rotation of the central axis around the z-axis, and Γ_ψ is the torque which results in the rotation of the cross-section around the central axis of the filament ($\Gamma < 0$ for an unwinding torque). Note that if the force has all three components (such as when fixing both ends of the rod), the term $f\cos\theta$ must be replaced by $\mathbf{f}\cdot\mathbf{t}$. We do not consider this much more complicated case because the force used in a force experiment is always uniaxial. Moreover, the torque may also be more complex and difficult to realize, so we stick to the simplest geometries. In a macroscopic experiment, one has often $\Gamma = 0$. In contrast, in a microscopic experiment, the torque has often a component along the direction of the stretching force.[13] In experiments, especially for biopolymers, one also often fixes the supercoiling degree[13] and in this case, we have $\Gamma = \Gamma_\psi$.[21,22]

In the absence of force and torque, it is obvious that the stable conformation of the filament, with $E = 0$, is given by

$$\omega_1 = \omega_{10}\,, \qquad \omega_2 = \omega_{20}\,, \quad \text{and} \quad \omega_3 = \omega_0\,. \quad (5)$$

These equations determine the free standing helix with constant curvature ($= \sqrt{\omega_{10}^2 + \omega_{20}^2}$) and constant torsion ($= \omega_0$), but the axis of the helix can point in any direction. For a free standing helix with its axis along the z-axis, we must have $\theta = \theta^H = \text{const.}$, $\phi = \dot{\phi}_h s$, so $\theta = \theta_0 = \tan^{-1}(\sqrt{\omega_{10}^2 + \omega_{20}^2}/\omega_0)$, $\psi = \psi_0 = \tan^{-1}(\omega_{10}/\omega_{20})$, $\dot{\phi}_h = \dot{\phi}_{h0} = \sqrt{\omega_{10}^2 + \omega_{20}^2 + \omega_0^2}$, $\kappa = \kappa_0 = \sqrt{\omega_{10}^2 + \omega_{20}^2}$, $\tau = \tau_0 = \omega_0$.

Extremizing E, we obtain the shape equations for a static filament,

$$a_1\ddot{\theta} + \frac{a_3 - a_1}{2}\sin 2\theta\dot{\phi}^2 + a_1(\omega_{20}\cos\psi + \omega_{10}\sin\psi)\dot{\psi}$$
$$+ \dot{\phi}[a_1\cos\theta(\omega_{20}\cos\psi + \omega_{10}\sin\psi) + a_3\sin\theta(\dot{\psi} - \omega_0)] - f\sin\theta = 0\,, \quad (6)$$

$$a_1\sin\theta(-\omega_{20}\cos\psi - \omega_{10}\sin\psi + \sin\theta\dot{\phi}) + a_3\cos\theta(-\omega_0 + \cos\theta\dot{\phi} + \dot{\psi}) - \Gamma = C\,, \quad (7)$$

$$a_3(\cos\theta\ddot{\phi} + \ddot{\psi}) + a_1\sin\theta(\omega_{10}\cos\psi - \omega_{20}\sin\psi)\dot{\phi}$$
$$- (a_1\omega_{20}\cos\psi + a_1\omega_{10}\sin\psi + a_3\sin\theta\dot{\phi})\dot{\theta} = 0\,. \quad (8)$$

Suppose the filament is fixed at one end ($s = 0$), the boundary conditions (BCs) at $s = 0$ are simply $\theta(0) = \theta_0$, $\phi(0) = \phi_0$ and $\psi(0) = \psi_0$. The extremum in the energy requires the following additional BCs at the other end ($s = L$),

$$\left(\frac{\partial\mathcal{E}}{\partial\dot{\theta}}\cdot\delta\theta\right)_{s=L} = \left(\frac{\partial\mathcal{E}}{\partial\dot{\phi}}\cdot\delta\phi\right)_{s=L} = \left(\frac{\partial\mathcal{E}}{\partial\dot{\psi}}\cdot\delta\psi\right)_{s=L} = 0\,, \quad (9)$$

or

$$[\dot{\theta}_L + \omega_{20}\sin\psi_L - \omega_{10}\cos\psi_L]\delta\theta_L = 0\,, \tag{10}$$

$$\begin{aligned}&\left[\frac{1}{2}(a_1 + a_3 + (a_3 - a_1)\cos 2\theta_L)\dot{\phi}_L + a_3\cos\theta_L(\dot{\psi}_L - \omega_0)\right.\\ &\qquad\left. - a_1\sin\theta_L(\omega_{20}\cos\psi_L + \omega_{10}\sin\psi_L) - \Gamma\right]\delta\phi_L = 0\,,\end{aligned} \tag{11}$$

$$[a_3(\cos\theta_L\dot{\phi}_L + \dot{\psi}_L - \omega_0) - \Gamma_\psi]\delta\psi_L = 0\,, \tag{12}$$

where $\psi_L = \psi(L)$, $\theta_L = \theta(L)$ and $\phi_L = \phi(L)$.

Equations (6)–(8) are nonlinear coupled differential equations which are very difficult to solve either analytically or numerically. However, it is easy to find analytic expressions for a helical filament.

3. Elasticity of a Helical Filament

3.1. *General expressions for a helix*

A helix with its axis along the z-direction of the fixed coordinate system can be expressed as

$$\mathbf{r} = \left\{\frac{\sin\theta^H}{\dot{\phi}_h}[1 - \cos(\dot{\phi}_h s)],\ \ -\frac{\sin\theta^H}{\dot{\phi}_h}\sin(\dot{\phi}_h s),\ \ \cos\theta^H s\right\}, \tag{13}$$

where $\dot{\phi}_h$ and θ^H are constants. The handedness of the helix is determined by the sign of $\dot{\phi}_h$. The radius of the helix is $a = \sin\theta^H/\dot{\phi}_h$, the torsion is $\tau = \dot{\phi}_h\cos\theta^H$, the curvature is $\kappa = \dot{\phi}_h\sin\theta^H$, and pitch is $p = 2\pi\cos\theta^H/\dot{\phi}_h$. The unit tangent vector of such a helix is therefore

$$\mathbf{t}^H = \{\sin(\dot{\phi}_h s)\sin\theta^H,\ -\cos(\dot{\phi}_h s)\sin\theta^H,\ \cos\theta^H\}\,. \tag{14}$$

From the requirements that a helix has constant curvature and torsion, McMillen and Goriely showed that in general a helix must have a constant ψ,[44] except for the WLRC model with $\omega_{10} = \omega_{20} = 0$. As a consequence, $\theta(s)$ and $\dot{\phi}(s)$ must also be constants, otherwise we have three differential equations but only two independent unknown functions $\theta(s)$ and $\dot{\phi}(s)$, so the problem becomes over-determined. Moreover, with ψ constant, we can show that under a non-uniaxial force, there is no helical solution for the shape equations, because the independent unknown functions in the shape equations will become $\theta(s)$ and $\phi(s)$. This is in fact resulted from the special BCs required by a helix which we will report in the following, i.e. one cannot fix $\theta(0)$ for a helix. These conclusions are also valid for a filament with non-circular cross-section.

Therefore, with $\theta(s) = \theta =$ constant, $\phi(s) = \dot{\phi}_h s$ with $\dot{\phi}_h$ also constant, and $\psi(s) = \psi =$ constant, the shape equations for a helix in this model can be reduced to

$$[a_1\cos\theta(\omega_{20}\cos\psi+\omega_{10}\sin\psi)-a_3\omega_0\sin\theta]\dot{\phi}_h+\frac{1}{2}(a_3-a_1)\sin 2\theta\dot{\phi}_h^2-f\sin\theta=0\,, \tag{15}$$

$$a_1\sin\theta(\dot{\phi}_h\sin\theta-\omega_{20}\cos\psi-\omega_{10}\sin\psi)+a_3\cos\theta(\dot{\phi}_h\cos\theta-\omega_0)-\Gamma=C\,, \tag{16}$$

$$\tan\psi=\frac{\omega_{10}}{\omega_{20}}\,. \tag{17}$$

Note that in this case, ψ is exactly the same as that of a free standing helix. For a helix, $z_{re}\equiv\cos\theta$ is equal to the relative extension and this is also an advantage of the use of Euler angles. Since excluded volume effects are not included, $z_{re}\le 0$ is allowed in this model. But $z_{re}<0$ is unphysical so we will not consider this case.

The twisted vertical line with $\Gamma=\Gamma_\psi=0$ is given by $\theta(s)=0$. It requires $\tan\psi=-\omega_{20}/\omega_{10}=\omega_{10}/\omega_{20}$, and it follows that $\omega_{10}=\omega_{20}=0$. This brings us back to the WLRC model.

In the general cases, for a helix, the BCs (10)–(12) become

$$[\omega_{20}\sin\psi_L-\omega_{10}\cos\psi_L]\delta\theta_L=0\,, \tag{18}$$

$$[\Gamma-a_1\sin\theta(-\omega_{20}\cos\psi-\omega_{10}\sin\psi+\dot{\phi}_h\sin\theta)-\ a_3\cos\theta(\dot{\phi}_h\cos\theta-\omega_0)]\delta\phi_L=0\,, \tag{19}$$

$$[a_3(\cos\theta_L\dot{\phi}_L-\omega_0)-\Gamma_\psi]\delta\psi_L=0\,. \tag{20}$$

BC (18) is automatically satisfied due to Eq. (17). But note that we have only one undetermined constant (C) in the shape equations for a helix, so the parts in bracket in Eqs. (19) and (20) cannot vanish simultaneously except for the WLRC model [see Eqs. (33)–(35)] or we can always keep $\Gamma_\psi=a_3(\cos\theta_L\dot{\phi}_L-\omega_0)$ which is uneasy in experiment, since otherwise it gives over-determined equations. Therefore, to have a helix, we have three kinds of possible BCs. The first kind of allowed BCs is

$$\Gamma-a_1\sin\theta(\dot{\phi}_h\sin\theta-\omega_{20}\cos\psi-\omega_{10}\sin\psi)-a_3\cos\theta(\dot{\phi}_h\cos\theta-\omega_0)=0\,, \tag{21}$$

$$\delta\psi_L=0\,. \tag{22}$$

$\delta\psi_L=0$ means that the ψ_L should be fixed. But since ψ is a constant for a helix, fixing ψ_L does not provide an additional constraint. To realize this condition, one simply does not fix the cross-section at both ends tightly on a non-deformable substrate but allows ψ to relax to the required value. This is also the BC used in some force experiments.[39]

The second kind of allowed BCs is

$$a_3(\cos\theta\dot{\phi}_h-\omega_0)-\Gamma_\psi=0\,, \tag{23}$$

$$\delta\phi_L=0\,. \tag{24}$$

$\delta\phi_L=0$ means that ϕ_L should be fixed and so $\dot{\phi}_h=(\phi_L-\phi_0)/L$ which would determine C. This condition is however difficult to realize since it requires fixing both $\phi(0)$ and $\phi(L)$ and may require additional and complicated applied forces and torques at both ends. In turn, the energy functional [Eq. (4)] may not be valid in this case. Therefore, we do not discuss the behavior of the helix given by BCs (23) and (24) in detail in this work.

The third kind of allowed BCs is

$$\delta\phi_L = 0 \quad \text{and} \quad \delta\psi_L = 0\,. \tag{25}$$

But it is easy to verify that replacing Γ by $\Gamma + C$, BCs (25) give exactly the same results as those given by BCs (21) and (22), so they are in fact equivalent. In the same way, we can show that to fix θ and ϕ at $s = 0$ is in fact unnecessary for a helix.

From Eqs. (15)–(17) and (21)–(22), we can obtain

$$\psi = \tan^{-1}\frac{\omega_{10}}{\omega_{20}}, \qquad \dot{\phi}_h = \frac{\Gamma + a_3 z_{re}\omega_0 + a_1\sqrt{1-z_{re}^2}\kappa_0}{a_1(1-z_{re}^2) + a_3 z_{re}^2}\,, \tag{26}$$

$$f = \frac{\begin{array}{c}[a_1 a_3\kappa_0 z_{re} - \sqrt{1-z_{re}^2}((a_1-a_3)\Gamma z_{re} + a_1 a_3\omega_0)] \\ \times(\Gamma + a_3 z_{re}\omega_0 + a_1\sqrt{1-z_{re}^2}\kappa_0)\end{array}}{\sqrt{1-z_{re}^2}[a_1(1-z_{re}^2) + a_3 z_{re}^2]^2}\,, \tag{27}$$

$$\mathcal{E}_{\text{helix}} = \frac{e_1}{2\sqrt{1-z_{re}^2}\kappa_0[a_1(1-z_{re}^2) + a_3 z_{re}^2]^2}\,, \tag{28}$$

$$\begin{aligned} e_1 = {} & -2a_1[(a_1 - 3(a_1-a_3)z_{re}^2 + 2(a_1-a_3)z_{re}^4)\Gamma \\ & - a_3 z_{re}^2(a_1(1-z_{re}^2) + a_3(z_{re}^2-2))\omega_0]\kappa_0^2 \\ & - \sqrt{1-z_{re}^2}\kappa_0[a_3 z_{re}^2\Gamma(3\Gamma + 4a_3 z_{re}\omega_0) \\ & + a_1^2 a_3(-(1-z_{re}^2)^2\omega_0^2 + z_{re}^2(1+z_{re}^2)\kappa_0^2) \\ & - a_1((3z_{re}^2-1)\Gamma^2 + 4a_3 z_{re}^3\Gamma\omega_0 + a_3^2 z_{re}^2((z_{re}^2-3)\omega_0^2 + z_{re}^2\kappa_0^2))]\,. \end{aligned} \tag{29}$$

It is clear that z_{re} may be a multi-valued function of f and Γ, and so is the energy. It means that the energy may be self-crossed, making abrupt changes in z_{re} possible. It is also interesting to note that Γ_ψ plays no role in forming a helix. This is simply because we cannot fix ψ_0, so applying a torque directly to the cross-section will result in a continuous rotation.

We should point out that there are many possible BCs for a filament, and different BCs may lead to different solutions. These BCs correspond to different constraints in experiment. Moreover, the results with different BCs are in fact not comparable directly. These important points are however often ignored in the study of the shape and stability of a filament. For instance, the simplest BCs are to fix two points only, but to allow the relaxation of θ, ϕ and ψ at both ends. In this case, the forces of both ends have in general all three components. One can further fix some angles which requires the application of a torque (or stress). In a force experiment, one usually applies a uniaxial force at one end. But even in this case, there are still different choices of BCs. For instance, if one fixes the initial tilting angle $\theta(0)$ but allows the relaxation of ϕ and ψ at both ends, then the rod can form a helix only in some special cases with f, Γ and Γ_ψ given by Eq. (27). For instance, if we fix $\theta(0)$ and Γ but vary f, then one can observe a helix only when $\theta(0)$, Γ and f satisfy Eq. (27). That often occurs in a macroscopic force experiment since it is relatively easy to fix $\theta(0)$, such as to clamp one end of the rod or to graft a small portion of rod at some fixed initial angle $\theta(0)$ to a substrate. However, in microscopic experiments, it is relatively easy to fix the initial position, but difficult to fix $\theta(0)$. Therefore, with the adjustable $\theta(0)$, at the microscopic level it should be easier to observe a helix under arbitrary force and torque.

With boundary conditions [Eqs. (21) and (22)], in general a static and slightly distorted helix cannot be formed in this model as an equilibrium configuration. This is because ψ will no longer be a constant, otherwise we will have three ordinary differential equations [Eqs. (6)–(8)], but only two variables [$\theta(s)$ and $\dot{\phi}(s)$]. Furthermore, if ψ is s-dependent, the condition $\delta\psi = 0$ cannot be used since it means that we need to fix both $\psi(0)$ and $\psi(L)$ and impose additional and complicated forces and torques at both ends. In turn, the energy functional [Eq. (4)] is not valid in this case. Therefore, for a non-helical shape, ψ should be s-dependent, and so from Eqs. (11) and (12), the BCs will become

$$\begin{aligned}&\frac{1}{2}\left[a_1 + a_3 + (a_3 - a_1)\cos 2\theta_L\right]\dot{\phi}_L + a_3\cos\theta_L(\dot{\psi}_L - \omega_0)\\&\qquad - a_1\sin\theta_L(\omega_{20}\cos\psi_L + \omega_{10}\sin\psi_L) - \Gamma = 0\,, \end{aligned} \tag{30}$$

$$a_3(\cos\theta_L\dot{\phi}_L + \dot{\psi}_L - \omega_0) - \Gamma_\psi = 0\,. \tag{31}$$

However, in general, a helix cannot satisfy these two BCs simultaneously. For instance, from Eqs. (26)–(28),

$$\begin{aligned}&a_3(z_{re}\dot{\phi}_h + \dot{\psi}_L - \omega_0) - \Gamma_\psi = \frac{D}{a_1(1 - z_{re}^2) + a_3 z_{re}^2}\,,\\&D \equiv a_1 a_3[\kappa_0 z_{re}\sqrt{1 - z_{re}^2} - \omega_0(1 - z_{re}^2)] + a_3 z_{re}\Gamma - [a_1(1 - z_{re}^2) + a_3 z_{re}^2]\Gamma_\psi\,.\end{aligned} \tag{32}$$

For a given filament, D vanishes only for some special values of z_{re}, with special f, Γ and Γ_ψ. That means a slightly distorted helix can only be formed around these special z_{re}. For instance, when $\Gamma = \Gamma_\psi = 0$, only the free-standing helix can satisfy both BCs so we can observe a nearly helical shape around a free-standing helix. But under arbitrary force and torque, in general, a static filament can be either a perfect helix or something far from a helix, but cannot be a slightly distorted helix. These conclusions are also correct for a filament with a non-circular cross-section. We should point out that we do not exclude the possibility of forming a slightly distorted helix dynamically, since dynamically, the energy of the system does not need to be minimum.

The helical solution with s-independent ψ for the WLRC model can be obtained from Eq. (26) by taking $\omega_{10} = \omega_{20} = 0$. ψ can be arbitrary in this case because the energy is independent of ψ. On the other hand, with $\omega_{10} = \omega_{20} = 0$, from Eqs. (6)–(12), we can find another helical solution for the WLRC model as

$$f = \frac{\Gamma\Gamma_\psi(1 + z_{re}^2) - (\Gamma^2 + \Gamma_\psi^2)z_{re}}{a_1(1 - z_{re}^2)}\,, \tag{33}$$

$$\phi(s) = \alpha s, \qquad \alpha = \frac{\Gamma - \Gamma_\psi z}{a_1(1 - z^2)}\,, \tag{34}$$

$$\psi(s) = \left(\omega_0 - z_{re}\alpha + \frac{\Gamma_\psi}{a_3}\right) s\,. \tag{35}$$

This solution allows a s-dependent ψ, but the force always decreases with increasing extension, so it should be not a stable solution and therefore we will not discuss it anymore.

3.2. *Stability criterion*

The helix obtained so far may be unstable since it may correspond to a maximum or a saddle point in energy. The stability (or at least metastability) of a rod requires

$$\delta^2 E = \int_0^L \left(\sum_{i,j=1,5} S_{ij}\delta\eta_i\delta\eta_j \right) ds > 0\,, \tag{36}$$

where $S_{ij} = \partial^2\mathcal{E}/\partial\eta_i\partial\eta_j$, with $\eta_1 = \theta$, $\eta_2 = \psi$, $\eta_3 = \dot{\phi}$, $\eta_4 = \dot{\theta}$, $\eta_5 = \dot{\psi}$. The positive (negative) definiteness of matrix S (with elements $S_{ij} = \partial^2\mathcal{E}/\partial\eta_i\partial\eta_j$, $i, j = 1, 5$) gives the sufficient condition for the stable (unstable) shape since it guarantees the validation (violation) of Eq. (36). Such a criterion may be very useful in some special case. However, it is not a necessary condition for the stability since η_4 and η_5 are not independent variables so S cannot determine the stability completely. This criterion is also too stringent for a helix because even under a very low force, the determinant of S would be negative.[45] It is also obvious that stability is boundary-condition-dependent.

For a helix, $\eta_4 = \eta_5 = 0$ and so a necessary condition for stability is the positive definiteness of matrix S' (with elements $S'_{ij} = \partial^2\mathcal{E}/\partial\eta_i\partial\eta_j$, $i, j = 1, 3$). This can be seen by noting that if we consider a simplified model with $\eta_4 = \eta_5 = 0$, we will obtain exactly the same shape equations but the corresponding stability will be completely determined by the positive definiteness of matrix S'. In other words, if all three eigenvalues of S' are positive, then the helix may be stable. Otherwise, if the three eigenvalues are all negative or do not have the same sign, the shape must be unstable. We cannot yet prove rigorously that it is also the sufficient condition for a stable helix, but at least it is robust because from it we can find that if the force increases with increasing extension, the helix will be stable, but if the force increases with decreasing extension, the helix will be unstable, in accordance with experimental observations. We should also be reminded that this criterion may be valid only for a helix.

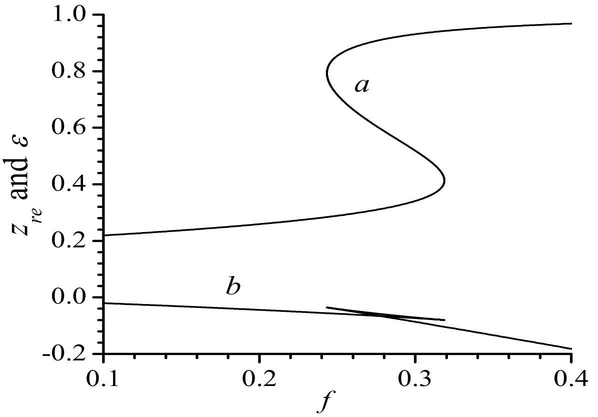

Fig. 1. Extension-force (curve a) and energy-force (curve b) relations for a helix. The parameters in figure are $\omega_0 = 0.09818 \times 10^5$ m^{-1}, $\kappa_0 = 0.50732 \times 10^5$ m^{-1}, $a_1 = 1.7797 \times 10^{-19}$ Nm^2, $a_3 = 18.686 \times 10^{-19}$ Nm^2, and $\Gamma = 0$. The units of f and $\mathcal{E}$ are 10^{-9} Newton. The elasticity of this helix agrees well with that observed for a helix in the CDLC.

For a free-standing helix, it can be shown exactly that all three eigenvalues of S' are positive so that the free-standing helix should be stable. This is what should be since the free-standing helix gives the minimum energy for the model.

Note that the positive definiteness of S' may only give a metastable conformation since under the same f and Γ, there may be several different solutions. A stable conformation requires a well-defined minimum in energy.

3.3. *Discontinuous extension transition for a helix under fixed torque*

This problem was tackled in a recent paper in a more general model of a rod with a non-circular cross-section (see Ref. 45). The most significant finding is that with proper parameters, a helical filament can be subject to a one-step first-order transition in z_{re} under a stretching force, and the corresponding energy-force curve is self-crossed, as shown in Fig. 1. The two tips in both the extension-force and energy-force curves define a metastable regime, in which the part on the right side of the cross-over point in energy corresponds to the jump in z_{re} with increasing force. In contrast, the part on the left side of the cross-over point of energy corresponds to the possible collapse of z_{re} with decreasing force. We find that increased twist rigidity, spontaneous curvature or decreased spontaneous torsion sharpens the transition of a helix under stretching. In contrast, a large bending rigidity favors a sharp transition under extension for a helix under compression. The role of the applied torque is complex. When the spontaneous curvature is small, under a small torque the sharpness of the transition is reduced but under a large torque the jump is favored. However, with a large spontaneous curvature, even a small torque favors a sharp transition. Hysteresis may be observed under decreasing force.

In view of the large parameter space to explore and the fact that the essential features are the same for a symmetric rod, it is advantageous to revisit the problem with the present model where three variables (θ or z_{re}, $\dot{\phi}$ and ψ) can be separated completely. In this model, one of the eigenvalues of S' can be found to be

$$\lambda_1 = \frac{a_1\omega_{20}\sqrt{1-z_{re}^2}(\Gamma + a_3\omega_0 z_{re} + a_1\omega_{20}\sqrt{1-z_{re}^2})}{a_3 z_{re}^2 + a_1(1-z_{re}^2)}\,. \tag{37}$$

It follows that a large negative Γ tends to destabilize the helix. The other two eigenvalues can also be written in closed form but the expressions are lengthy so we do not present them here. A new finding with this model is that if $a_1 \gg a_3$ and under compressive force (i.e. $f < 0$), there may also be a one-step transition of z_{re}. Our calculations show further that df/dz_{re} always shares the same zeroes with one of the eigenvalues of S', and the regime with $df/dz_{re} < 0$ always overlaps with the regime having negative eigenvalues. It means that the regime with $df/dz_{re} < 0$ is always unstable, as common sense would suggest. In contrast, in most cases, the regime with $df/dz_{re} > 0$ is stable or at least metastable. Furthermore, we find that in most cases, there is only one eigenvalue which can change sign as f is varied, so the unstable points are saddle points. Besides the metastable regime mentioned in the first paragraph of this section, $df/dz_{re} < 0$ in general occurs for large negative torques or strong compressive forces.

Moreover, from Eq. (27), when $z_{re} \to 1$,

$$f \to \frac{a_3\Gamma(\Gamma + a_3\omega_0) - a_1(\Gamma + a_3\omega_0)^2 + a_1^2 a_3\kappa_0^2}{a_3^2} + \frac{a_1(\Gamma + a_3\omega_0)\kappa_0}{a_3\sqrt{1-z_{re}^2}}\,. \tag{38}$$

It follows that except for $(\Gamma + a_3\omega_0)\kappa_0 = 0$, to stretch a helix to its full length requires infinite force. As a consequence, a helix with $(\Gamma + a_3\omega_0)\kappa_0 = 0$ may have quite a different behavior. In the special case with $\omega_0 = 0$ and $\Gamma = 0$, we can find that

$$\frac{df}{dz} = \frac{a_1^2 a_3\kappa_0^2[a_1 + 3(a_1 - a_3)z_{re}^2]}{[a_1(1-z_{re}^2) + a_3 z_{re}^2]^3} > 0\,. \tag{39}$$

Therefore, in this case, the force increases monotonically with increasing z_{re}, so that there is no sharp jump in z_{re} of the helix. This gives another very important reason why one cannot observe the sharp jump of extension for most macroscopic helical springs since a macroscopic helical spring in general has very small or even vanishing spontaneous torsion, and in general in experiment $\Gamma = 0$. Such phenomena should be observable in the material having screw axes since it corresponds to an intrinsic torsion, but such materials are in general not appropriate for a macroscopic spring. However, many microscopic objects have spontaneous twisting. Therefore, it should be easier to observe a sharp jump in the extension in microscopic objects. But if $\Gamma \neq 0$, one may still observe the sharp change of z_{re} even with $\omega_0 = 0$.

It has been reported that under a stretching force, a helix in a CDLC, which is produced in the process of cholesterol crystallization in the native gallbladder bile, can undergo a one-step reversible sharp transition in the relative extension z_{re}

from an almost perfect helix to an almost straight line ($z_{re} = 1$),[39] and there is a metastable regime, $z_{re} = 0.28$ to $z_{re} = 0.41$ (note that the pitch angle ψ in Ref. 39 is the same as $\pi/2 - \theta$ in this work), in which upon nucleation, the helix separates into two domains, one straight and the other helical ($z_{re} = 0.28$). Reference 39 also constructed a free energy model to account for the phenomena. However, we find that our model is enough to predict these experimental observations. We can first note that in this model, z_{re} is essentially one, or the helix becomes a straight line in the stretched regime. By expanding around $z_{re}^0 = \cos\theta_0 = \omega_0/|\dot{\phi}_{h0}|$ and up to the first-order, we get $f = k(z_{re} - z_{re}^0)$, where $k = a_1 a_3 |\dot{\phi}_{h0}|^6/(a_1\kappa_0^4 + a_3\kappa_0^2\omega_0^2)$ is the spring constant. We use the radius $R_0 = 19$ μm, $z_{re} = z_{re}^0 = 0.19$ of the free-standing helix, and the spring constant reported ($= 4.8 \times 10^{-6}\mathrm{Nm}^{-1}$) to remove three of the four parameters in our model, and use a_3/a_1 as the unique parameter to fit to the right tip of the sharp edge (given by $df/dz_{re} = 0$ with $z_{re} \approx 0.41$) in the extension-force curve, and find that $a_1 = 1.7797 \times 10^{-19}$ Nm^2, $a_3 = 18.686 \times 10^{-19}$ Nm^2, $\omega_0 = 0.09818 \times 10^5$ m^{-1}, $\kappa_0 = 0.50732 \times 10^5$ m^{-1}, and also recover the solution obtained in Ref. 45. This solution gives the cross-over point of energy at $z_{re} = 0.278$ and the right tip of the sharp edge of the extension-force curve at $z_{re} = 0.413$. These two bounds provide a perfect agreement with the observed metastable regime. Moreover, due to the self-crossing in the energy-force curve, the two-domain (one straight and the other helical) coexistence is possible around the cross-over point, especially if one considers thermal fluctuation, as observed in experiment.[39]

Another interesting case would be the behavior of the short dsDNA chain under low torque since it can be described by the WLRC model, although to keep a non-vanishing torque in experiment may be difficult due to the special requirement on the boundary conditions. For the WLRC model, we do not find the sharp change in the extension. Furthermore, if $a_1 > a_3$, we can show $df/dz_{re} < 0$ exactly so the helix is unstable. For the dsDNA, we have $a_1 = 53$ nm k_BT, $a_3 = 75$ nm k_BT, $\omega_0 = 2\pi/(10.5 \times 0.34)$ nm^{-1}, k_B is the Boltzmann's constant and T is the temperature. In this case, we find that when $\Gamma = 0$, $df/dz_{re} > 0$ requires $z_{re} > 0.8961$, which means that the helix can be stable only at a large extension. Negative torque tends to make the helix unstable, but the positive tends to stabilize the helix. We should be reminded that the helix for the dsDNA here represents the shape of the axial line of the dsDNA, and is different from the shape of the backbones which is intrinsically the double-stranded helix. We should also note that the long dsDNA chain is not a proper object because it will be subjected to serious thermal fluctuation.

3.4. *Elasticity of a helical filament under constant force*

$f = 0$ is special. In this case, from Eq. (27), we get

$$\Gamma = -a_3 z_{re}\omega_0 - a_1\sqrt{1 - z_{re}^2}\,\kappa_0\,, \tag{40}$$

$$\text{or} \qquad \Gamma = \frac{a_1 a_3(\kappa_0 z_{re} - \omega_0 \sqrt{1 - z_{re}^2})}{(a_1 - a_3) z_{re} \sqrt{1 - z_{re}^2}} \,. \tag{41}$$

But Eq. (40) leads to $\dot{\phi}_h = 0$ so it is not a helical solution. From Eq. (41), in this case, $z_{re} = 0$ and $z_{re} = 1$ all require an infinite Γ and energy. It can be shown that $d\Gamma/dz_{re}$ has the same sign as $a_1 - a_3$, so z_{re} is a monotonous function of Γ and therefore there is no sharp jump of z_{re} in this case.

When $f \neq 0$, we can show that

$$\Gamma = \Gamma_{1,2} = \frac{A \pm [a_1(1 - z_{re}^2) + a_3 z_{re}^2]\sqrt{B}}{2(a_1 - a_3) z_{re} \sqrt{1 - z_{re}^2}} \,, \tag{42}$$

$$\begin{aligned} A &= a_3^2 \omega_0 z_{re}^2 \sqrt{1 - z_{re}^2} - a_1^2 \kappa_0 z_{re}(1 - z_{re}^2) \\ &\quad - a_1 a_3[\omega_0 \sqrt{1 - z_{re}^2}(1 + z_{re}^2) - \kappa_0 z_{re}(2 - z_{re}^2)], \\ B &= a_3^2 \omega_0^2 (1 - z_{re}^2) - 2 a_1 a_3 \omega_0 \kappa_0 z_{re} \sqrt{1 - z_{re}^2} \\ &\quad + z_{re}[4(a_1 - a_3) f (z_{re}^2 - 1) + a_1^2 \kappa_0^2 z_{re}] \,, \end{aligned} \tag{43}$$

where the $+$ in the numerator of Eq. (42) corresponds to Γ_1. Note that $\Gamma_1 = \Gamma_2$ when $B = 0$. B may be always positive in the interval $1 > z_{re} > 0$ and in this case, the relationship between z_{re} and Γ is separated into two disjointed segments given by Γ_1 and Γ_2 respectively. Moreover, when B has zeros in the interval $1 > z_{re} > 0$, our calculations show that B has in general two zeros except in the case with $\omega_0 = 0$, and it follows that the relationship between z_{re} and Γ is also separated into two disjointed segments. However, the stability analysis shows that the left segment (i.e. with large negative torque) is always unstable, so we will not discuss it anymore. This result agrees with those reported in the Sec. 3.3. When $\omega_0 = 0$, we can show exactly that B has at most one zero in the interval $1 > z_{re} > 0$.

One of eigenvalues of S' can be found to be

$$\lambda_{1\pm} = \frac{a_1 \kappa_0 (a_1 \kappa_0 z_{re} - a_3 \omega_0 \sqrt{1 - z_{re}^2} \pm \sqrt{B})}{2(a_1 - a_3) z_{re}} , \tag{44}$$

where the $+$ corresponds to Γ_1. From Eq. (44), we find that when $z_{re} \to 0$, $\lambda_{1+} \to -a_1 \kappa_0 f/(a_3 \omega_0)$, $\lambda_{1-} \to a_1 a_3 \omega_0 \kappa_0/(a_3 z_{re} - a_1 z_{re})$. When $z_{re} = 1$, $\lambda_{1+} = a_1^2 \kappa_0^2/(a_1 - a_3)$, $\lambda_{1-} = 0$. As a consequence, if $a_3 < a_1$, $\lambda_{1-} < 0$ when z_{re} closes to zero, then the helix given by Γ_2 is unstable in $z_{re} \sim 0$. If $a_3 > a_1$, $\lambda_{1+} < 0$ when z_{re} closes to one, then the helix given by Γ_1 is unstable in $z_{re} \sim 1$. Moreover, if $f > 0$, $\lambda_{1+} < 0$ when z_{re} closes to zero, then the helix given by Γ_1 is also unstable in $z_{re} \sim 0$.

From Eq. (42), we find that if $a_3 > a_1$ and $f > 0$, when f and a_3 are both small, the z_{re} is in general a two-valued function of Γ, and the two branches are separated by a minimum torque, Γ_m (with $z_{re} = z_{re}^m$), as shown in the curve (a) of Fig. 2 and the solid line of Fig. 3. However, we find that the upper part with $z_{re} > z_{re}^m$ and $d\Gamma/dz > 0$ has always a higher energy than the part with $z_{re} < z_{re}^m$ under the same Γ, so the upper part is unstable, and the stability analysis using S' gets the

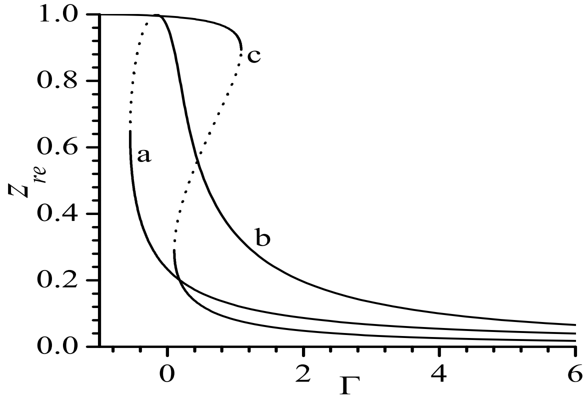

Fig. 2. Typical extension-torque relation of a helix under constant force. The parameters are (a) $\omega_0 = 0.1$, $\kappa_0 = 1$, $a_1 = 1$, $a_3 = 1.5$ and $f = 0.2$. (b) The same as (a) except for $f = 1$. (c) The same as (b) except for $a_3 = 10$. The left segment of each curve is not plotted since the corresponding shape is unstable. The dotted lines indicate the unstable regime. Γ has the same units as $a_1\kappa_0$.

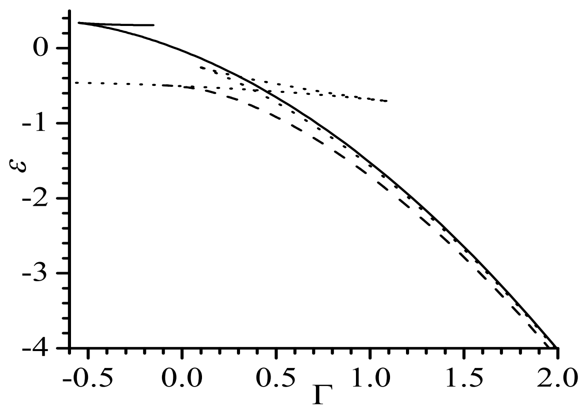

Fig. 3. Energy versus torque Γ for a helix corresponds to Fig. 2. The solid line corresponds to curve (a) in Fig. 2, the dashed line corresponds to curve (b) in Fig. 2, the dotted line corresponds to curve (c) in Fig. 2. The units of energy per unit length are those of $a_1\kappa_0^2$, while for Γ they are those of $a_1\kappa_0$.

same conclusion. Therefore, in fact the z_{re} of right segment decrease monotonically with increasing Γ, so that no jump in z_{re} can occur. It also suggests that a helix is prohibited in large z_{re}. Increasing f makes the z_{re} decrease monotonically with increasing Γ, as shown in the curve (b) of Fig. 2 and dashed line of Fig. 3. Large a_3 and f may lead to a jump or collapse in z_{re}, as shown in the curve (c) of Fig. 2 and the dotted line of Fig. 3. In this case, z_{re} decreases with increasing Γ until a local maximum Γ, in which the z_{re} may collapse with further increase in Γ. A hysteresis

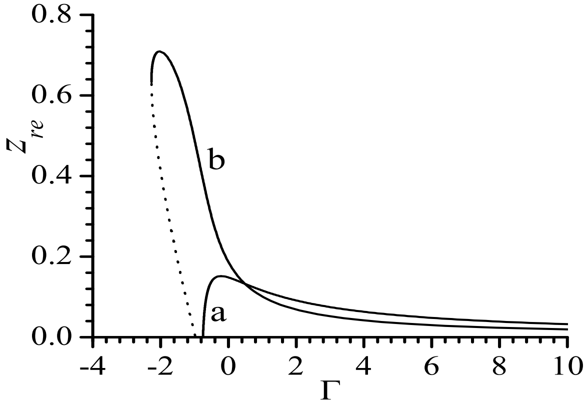

Fig. 4. Typical extension-torque relation of a helix under constant force. The parameters in the curve (a) are $\omega_0 = 0.2$ and $\kappa_0 = 1$, $a_1 = 1$, $a_3 = 2$ and $f = -0.1$. The parameters in the curve (b) are the same as (a) except for $a_3 = 15$. The left segment of each curve is not plotted since the corresponding shape is unstable. The dotted lines indicate the unstable regime. Γ has the same units as $a_1\kappa_0$.

may also be observed if Γ decreases from a large value. From stability analysis using S', we find again that the regime with $d\Gamma/dz > 0$ is always unstable.

If $a_3 > a_1$ and $f < 0$, we find that there is no sharp jump in z_{re}. When a_3 and ω_0 are both small, z_{re} is a single-valued (but not monotonic) function of Γ, as shown in the curve (a) of Fig. 4. When a_3 is large but ω_0 is small, the z_{re} of the right segment is a two-valued function of Γ with a minimum torque, Γ_{1m} (and $z_{re} = z_{re}^m$), as shown in the curve (b) of Fig. 4. However, the part with $z_{re} > z_{re}^m$ has always a lower energy so that the part with $z_{re} < z_{re}^m$ is in fact inaccessible. The stability analysis using S' supports this conclusion again. Therefore, z_{re} is again a single-valued (but not monotonic) function of Γ.

If $a_1 > a_3$ and $f > 0$, when f is small, the z_{re} of the right segment is again a two-valued function of Γ, as shown in the curve (a) of Fig. 5. However, we find that the part with $z_{re} > z_{re}^m$ has always a higher energy than the part with $z_{re} < z_{re}^m$ with the same value of Γ, and so is unstable. Therefore, in this case, the z_{re} value of the right segment is in fact a single-valued (but not monotonic) function of Γ. Increasing f makes the z_{re} value of the right segment a monotonic function of Γ, as shown in the curve (b) of Fig. 5.

If $a_1 > a_3$ and $f < 0$, and when ω_0 is small or under large $|f|$, the z_{re} value of the right segment becomes a two-valued function of Γ, as shown in the curve (c) of Fig. 5, but the part with $z_{re} < z_{re}^m$ has in general a higher energy than the part with $z_{re} > z_{re}^m$, and so is unstable. Hence, the z_{re} value of the right segment is in fact a monotonic function of Γ. A stability analysis using S' supports this conclusion.

The relationship between z_{re} and Γ with fixing f can be summarized in Table 1. We find that negative torque tends to make the helix unstable, and when $a_3 > a_1$,

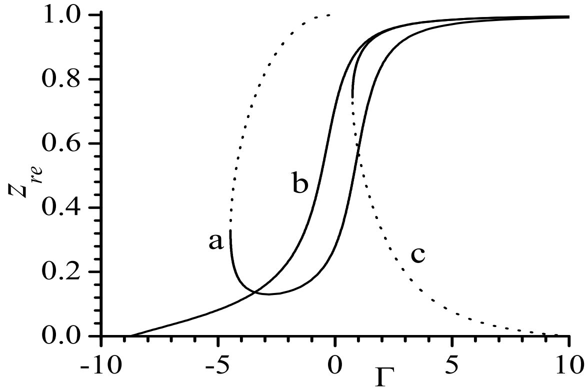

Fig. 5. Typical extension-torque relation of a helix under constant force. The parameters in (a) are $\omega_0 = 0.2$, $\kappa_0 = 1$, $a_1 = 5$, $a_3 = 1$ and $f = 0.1$. The parameters in (b) are: $\omega_0 = 1.2$, $\kappa_0 = 1$, $a_1 = 15$, $a_3 = 1$ and $f = -0.5$. The parameters in (c) are the same as (b) except for $f = -2$. The left segment of each curve is not plotted since the corresponding shape is unstable. Γ has the same units as $a_1\kappa_0$.

Table 1. Trends in the variation of z_{re} as a function of Γ with fixing f.

	$a_3 > a_1$	$a_3 < a_1$
$f > 0$	Monotonically except for large a_3, f and small ω_0.	If f is small, single valued but not monotonic. If f is large, monotonic.
$f < 0$	Single valued but not monotonic.	Monotonic.

and ω_0 is small, and a_3 and f are large, there may be a sharp change in z_{re} because the z_{re} value can be trivalued functions of Γ. Otherwise the z_{re} values of the helix are in fact single-valued functions of Γ, and no sharp change in z_{re} can occur.

Whether the behaviors reported in this section are observable in experiments is an intriguing question. We have to say that due to the special requirements of the boundary conditions, the relevant experiments may be difficult. The short dsDNA chain under low torque which can be represented by the WLRC model, and the helix in a CDLC are likely candidates to observe these predictions. We expect that such experiments would give some important insights on the elastic properties of these biopolymers as well as on how appropriate the elastic model is for describing these biopolymers. For the WLRC model, we do not find a sharp change in the extension. Furthermore, we find that at the same z_{re}, the helix given by Γ_2 has always a lower energy than that with Γ_1, so only the helix given by Γ_2 is observable. Moreover, if $a_1 > a_3$ or $d\Gamma/dz > 0$, the helix is always unstable so that the extension of a helix decreases monotonically with increasing torque.

The more interesting case should be the elastic property of the helix in a CDLC because we can predict a sharp transition of z_{re} under a moderate stretching force. Using the parameters given in Sec. 3.3, we find that when $f > 0.155 \times 10^{-9}$ N, there will be an abrupt change of extension for a helix under twisting. This follows from the expression given by Γ_2 and it has a similar behavior as shown in curve (c) of Fig. 2. Moreover, the two-domain (one straight and the other helical) coexistence is also possible due to the self-crossing in the energy–torque curve. In contrast, in this case, the helix given by Γ_1 is always unstable.

4. Concluding Remarks

In summary, we derive the shape equations in terms of Euler angles for an elastic rod with spontaneous twist and curvatures and with isotropic bending rigidity. We find the boundary conditions required to form a helical filament in a force experiment. Due to the stringent requirements of the boundary conditions, we show that in static state, there is no nearly helical solution in the model in a force experiment except for some special cases. Besides these special cases, the observed nearly helical shapes should be due to the non-uniformity of the filament, or the effect of thermal fluctuations which allow the exploration of non-equilibrium structures near the minimum energy configuration dynamically. We present in detail the closed form expressions for the helical solution and study the elasticity and stability of the helical ribbon under different conditions of stretch and twisting. We find that the extension of a helix may be subject to a one-step sharp transition when using the torque as the independent variable. This agrees quantitatively with experimental observations for a stretched helix in a chemically-defined lipid concentrate.[39] More specifically, the sharp transition in extension z_{re} in a helix may occur when the twisting rigidity a_3 is larger than the bending rigidity a_1 and the spontaneous twist rate ω_0 is small, or when $a_3 > a_1$ with both a_3 and the applied stretching force f large, or $a_1 \gg a_3$ but under a compressive force. We predict further that the extension of the helix in a CDLC may have an abrupt transition if it is subject to a variable torque and a fixed stretching force. As mentioned above, our results also show that there is no multiple-step transition of the extension[37] for a perfect helix under stretching. We believe that a multiple-step transition can occur only for a distorted helix. We also find that a strong negative torque always makes the helix unstable.

Although the shape equations we derived are very general, we focus on the simplest helical solutions in this work. In practice, a helical filament under force and torque may be unstable and transform into other complicated shapes.[9,10,43,44] The conditions of the transition and the relevant stability, both static and dynamical, of the different shapes are in themselves intriguing issues. In this paper, we do not consider thermal effects. Due to the self-crossing in the energy-force curve, the direct effect of the temperature is to make the coexistence of the two domains (one straight and the other helical) possible, as observed in experiment.[39] Another important effect is a contraction of the rod due to configurational entropy, which is analogous to a compressive force for a long rod, and it may make the transition smoother. Therefore, it is reasonable to expect that the main characteristics of our work, such as a first-order transition in the extension, should still be observed even at finite temperature. Moreover, the conformational information so obtained should be useful even in the case that entropic effects dominate, since energetics are a crucial component in determining the most likely conformations.

Acknowledgments

This work has been supported by the National Science Council of the Republic of China under Grant nos. NSC 93-2112-M-032-006, NSC 94-2119-M-032-010, and the Natural Sciences and Engineering Research Council of Canada.

References

1. A. E. H. Love, *A Treatise on the Mathematical Theory of Elasticity* (Dover, New York, 1944).
2. L. D. Landau and E. M. Lifshitz, *Theory of Elasticity*, 3rd ed. (Pergamon, 1986).
3. S. Iijima, *Nature* (*London*) **354** (1991) 56; S. Iijima, T. Ichihaschi and Y. Ando, *ibid.* **356** (1992) 776.
4. M. S. Dresselhaus, *Nature* (*London*) **3548** (1992) 195.
5. X. B. Zhang, *Europhys. Lett.* **27** (1994) 141.
6. Z.-C. Ou-Yang, Z.-B. Su and C.-L. Wang, *Phys. Rev. Lett.* **78** (1997) 4055.
7. M.-F. Yu, M. J. Dyer, J. Chen, D. Qian, W. K. Liu and R. S. Ruoff, *Phys. Rev. B* **64** (2001) 241403.
8. A. F. da Fonseca and D. S. Galvão, *Phys. Rev. Lett.* **92** (2004) 175502.
9. A. Goriely and M. Tabor, *Phys. Rev. Lett.* **80** (1998) 1564.
10. R. E. Goldstein, A. Goriely, G. Huber and C. W. Wolgemuth, *Phys. Rev. Lett.* **84** (2000) 1631.
11. D. Coombs, G. Huber, J. O. Kessler and R. E. Goldstein, *Phys. Rev. Lett.* **89** (2002) 118102.
12. S. B. Smith, L. Finzi and C. Bustamante, *Science* **258** (1992) 1122.
13. T. R. Strick, J. F. Allemand, D. Bensimon, A. Bensimon and V. Croquette, *Science* **271** (1996) 1835.
14. P. Cluzel, A. Lebrun, C. Heller, R. Lavery, J. L. Viovy, D. Chatenay and F. Caron, *Science* **271** (1996) 792.
15. S. B. Smith, Y. Cui and C. Bustamante, *Science* **271** (1996) 795.
16. J. F. Léger, G. Romano, A. Sarkar, J. Robert, L. Bourdieu, D. Chatenay and J. F. Marko, *Phys. Rev. Lett.* **83** (1999) 1066.
17. T. R. Strick, V. Croquette and D. Bensimon, *Proc. Natl. Acad. Sci. USA* **95** (1998) 10579.
18. C. J. Benham, *Proc. Natl. Acad. Sci. USA* **74** (1977) 2397.
19. F. Tanaka and H. Takahashi, *J. Chem. Phys.* **83** (1985) 6017.
20. C. J. Benham, *Phys. Rev. A* **39** (1989) 2582.
21. B. Fain and J. Rudnick, *Phys. Rev. E* **60** (1999) 7239.
22. H. Zhou, Y. Zhang and Z.-C. Ou-Yang, *Phys. Rev. Lett.* **82** (1999) 4560.
23. B. Fain, J. Rudnick and S. Östlund, *Phys. Rev. E* **55** (1997) 7364.
24. J. F. Marko and E. D. Siggia, *Science* **265** (1994) 506.

25. C. Bustamante, J. F. Marko, E. D. Siggia and S. Smith, *Science* **265** (1994) 1599.
26. J. F. Marko and E. D. Siggia, *Macromolecules* **28** (1995) 8759.
27. J. F. Marko and E. D. Siggia, *Phys. Rev. E* **52** (1995) 2912.
28. J. F. Marko, *Phys. Rev. E* **55** (1997) 1758.
29. J. F. Marko, *Europhys. Lett.* **38** (1997) 183; *Phys. Rev. E* **57** (1998) 2134.
30. C. Bouchiat and M. Mézard, *Phys. Rev. Lett.* **80** (1998) 1556.
31. C. Bouchiat and M. Mézard, *Euro. J. Phys. E.* **2** (2000) 377.
32. S. Panyukov and Y. Rabin, *Phys. Rev. Lett.* **85** (2000) 2404.
33. S. Panyukov and Y. Rabin, *Phys. Rev. E* **62** (2000) 7135.
34. S. V. Panyukov and Y. Rabin, *Phys. Rev. E* **64** (2001) 011909.
35. Y. Kats, D. A. Kessler and Y. Rabin, *Phys. Rev. E* **65** (2002) 020801.
36. S. V. Panyukov and Y. Rabin, *Europhys. Lett.* **57** (2002) 512.
37. D. A. Kessler and Y. Rabin, *Phys. Rev. Lett.* **90** (2003) 024301.
38. J. D. Moroz and P. Nelson, *Proc. Natl. Acad. Sci. USA* **94** (1997) 14418.
39. B. Smith, Y. V. Zastavker and G. B. Benedek, *Phys. Rev. Lett.* **87** (2001) 278101.
40. Y. Cui and C. Bustamante, *Proc. Natl. Acad. Sci. USA* **97** (2000) 127.
41. M. Hegner, S. B. Smith and C. Bustamante, *Proc. Natl. Acad. Sci. USA* **96** (1999) 10109.
42. K. Cahill, *Phys. Rev. E* **72** (2005) 062901.
43. A. Goriely and M. Tabor, *Proc. R. Soc. London A* **453** (1997) 2583.
44. T. McMillen and A. Goriely, *J. Nonlinear Sci.* **12** (2002) 241.
45. Z. Zhou, P.-Y. Lai and B. Joós, *Phys. Rev. E* **71** (2005) 052801.
46. H. Goldstein, *Classical Mechanics*, 3rd edn. (Addison-Wesley, 2002).